Implications of Stress-Drop Models of Earthquakes for the Inversion of Stress Drop from Seismic Observations

Article *in* Pure and Applied Geophysics · November 1977

DOI: 10.1007/BF01637111

CITATIONS
69

READS
86

1 author:

Raúl Madariaga
Ecole Normale Supérieure de Paris
277 PUBLICATIONS **12,782** CITATIONS

SEE PROFILE

Pageoph, Vol. 115 (1977), Birkhäuser Verlag, Basel

Implications of Stress-Drop Models of Earthquakes for the Inversion of Stress Drop from Seismic Observations

By RAUL MADARIAGA[1])

Abstract – We discuss the inversion of stress drops from seismic observations on the basis of crack or stress-drop models of earthquake mechanism. Since a formal inverse problem cannot be posed at present we discuss implications of solutions to direct problems. We first discuss the static approximations used to obtain stress drop from seismic moment and source dimensions. We show that the geometrical effects are quite significant if only one source dimension has been retrieved from seismic observations. The effect of variable stress drop is discussed and we show that the inverted stress drop is not a simple average of the actual stress drops on the fault. We discuss the energy release during faulting and show that the apparent stress has a complicated relation to the stress drop on the fault. We also show that the static stress drops obtained by seismologists are a lower bound to the actual dynamic stress drops on the fault. This may in part explain disagreements with laboratory results. Finally, we discuss the inversion of source dimensions from the far-field radiation. We analyse two extreme, simple dynamical source models, a circular fault and a rectangular fault and show that geometry has a much more pronounced effect on radiation than is usually acknowledged.

Key words: Stress drop; Earthquake source theory; Earthquake source dimension.

1. Introduction

The number of stress drop determinations from seismic observations of earthquakes has increased substantially in recent years thanks both to developments in the study of the velocity and density structure of the earth and to the general acceptance of earthquake models based on the slip (dislocation) on a fault plane. Reviews of some of the available data may be found in KANAMORI and ANDERSON (1975) for large earthquakes $M_s > 7$ and in THATCHER and HANKS (1973) for determinations of stress drops for California earthquakes. These studies determine average stress drop, average effective stress or average apparent stress. A question naturally arises as to the exact meaning of these averages and how well can they be determined in the presence of complicating factors such as variable stress, variable rupture velocity, source geometry, etc. These questions properly pertain to the inverse problem of the earthquake source. Suppose we have been able to completely correct for the effects of propagation and attenuation (a very difficult task itself) and we want to find the geometry, stress drop distribution and rupture history of the earthquake. Such a formal inverse problem may not be considered at the present time because we do

[1]) Department of Earth and Planetary Sciences, Massachusetts Institute of Technology, Cambridge, MA 02139, USA.

not know enough about the direct problem. In fact, only a few extremely simplified three dimensional fault models have been numerically solved for the direct problem (MADARIAGA, 1976, 1977, CHERRY *et al.*, 1976, ARCHULETA and FRAZIER, 1976). We will therefore content ourselves with a discussion of inferences made from the experience obtained solving these very simplified source models.

In the first section we discuss the usual method to find stress drop from seismic moment and source area observations. We shall discuss the influence of source geometry and what kind of average is usually found when the stress drop is variable on the fault. Next we discuss seismic energy radiation which is a convenient way to introduce boundary conditions at the fault and discuss the relation between the frictional law on the fault and the seismic energy. In the last section we consider the effect of geometry on the seismic radiation and spectra in the far-field. The discussion of two simple models; a circular and a rectangular fault, serves to emphasize the significant effect of geometry on the seismic radiation and the inversion of stresses.

2. *Static parameters*

The most important static parameter that may be obtained from seismic observations is the seismic moment. In the far-field, and at periods much longer than the source size, a fault appears as a point double couple source. The scalar value of the moment of one of these couples is the seismic moment (AKI, 1966). The seismic moment is related to the final slip D at the fault by the following relation (BURRIDGE and KNOPOFF, 1964).

$$M_0 = \mu \int_S dS\, D(x, y) \tag{1}$$

where μ is the rigidity of the elastic medium surrounding the fault and S is the final area of the fault. It is frequently rewritten in the form

$$M_0 = \mu \bar{D} S \tag{2}$$

where $\bar{D}$ is the average final slip at the fault.

In order to obtain the stress drop from the seismic moment we need a relation between $\bar{D}$ and the stress drop $\Delta\sigma$ on the fault. Seismologists usually assume that the stress drop on the fault is constant and then compute the average slip for different geometries (circular or two-dimensional plane and antiplane). Posed in this form the problem is that of a shear crack under uniform stress drop, i.e., uniform difference between tectonic and frictional stresses. The solution to this problem may be written in the general form

$$\bar{D} = C \frac{\Delta\sigma}{\mu} W \tag{3}$$

where W is a characteristic length associated with the *narrowest* dimension of the fault. For circular faults it is the radius, for elliptical faults the semi-minor axis, for long faults its half width. The coefficient C is a form factor that depends on the geometry of the fault and the direction of slip.

For an elliptical fault of semi-major axis L and semi-minor axis W we may find C using some results, of ESHELBY (1957). For transversal slip, i.e., for slip in the direction W we find

$$C = 4/\left[3E(k) + \frac{w^2}{L^2}(K(k) - E(k))/k^2\right] \tag{4}$$

where $k = (1 - W^2/L^2)^{1/2}$ and $K(k)$ and $E(k)$ are complete elliptical integrals. Similarly, for longitudinal slip (along the semi-major axis) we find

$$C = 4/\left[3E(k) + (E(k) - \frac{w^2}{L_2}K(k))/k^2\right] \tag{5}$$

Both in (5) and (4) we have assumed that the Poisson ratio $v = 0.25$. When $L = W = R$ (circular fault) we find $C = 16/7\pi = 0.728$ a result obtained by KEILIS BOROK (1959). This is the minimum value of C from (4) or (5). On the other hand for a very long, rectangular, longitudinal slip fault $C = \pi/2 = 1.57$ as shown by KNOPOFF (1958). This value of C is larger than C for any elliptical fault and it is quite probably the maximum possible value for any fault geometry. For a transversal slip long fault we find the intermediate value $C = 3\pi/8 = 1.18$. Thus it appears that C varies at most by a factor of two for different source geometries.

Combining (3) and (1) we find the stress drop

$$\Delta\sigma = \frac{M_0}{CSW} \tag{6}$$

Thus, if we know M_0, S and W, the stress drop $\Delta\sigma$ may be found with a precision better than a factor of at most two. However, in most cases, only one size parameter is obtained from seismic observations via the corner frequency (see section 4). In that case (6) is frequently replaced by the rough approximation

$$\Delta\sigma = \frac{M_0}{CS^{3/2}} \tag{7}$$

which is obviously a poor approximation for long thin faults and may produce errors much larger than a factor of two.

Thus far we have assumed a constant stress drop on the fault, which is quite unlikely in earthquakes since we expect substantial variation of both the initial tectonic stress field and the final frictional stress. In such cases we have to replace $\Delta\sigma$ in (3), (6) or (7) by a certain weighted average $\Delta\sigma^*$ of the stress drop on the fault. In order to find an expression for $\Delta\sigma^*$ for faults of general shape we would have to solve a difficult crack problem with variable stress. However, we can get an estimate

of the effect of variable stress drop studying a simpler plane fault model. A solution for the slip on a plane fault due to a general stress drop was found by SNEDDON and LOWENGRUB (1969, pp. 25–35). Averaging their results yields the following expression for the average slip on the fault

$$\bar{D} = C \frac{2}{\mu \pi W} \int_{-W}^{W} \Delta\sigma(x) \sqrt{W^2 - x^2}\, dx$$

where x is the coordinate along the fault. Thus, the weighted average stress drop is

$$\Delta\sigma^* = \frac{2}{\pi W^2} \int_{-W}^{W} \Delta\sigma(x) \sqrt{W^2 - x^2}\, dx \tag{8}$$

We have designated this average with a star to indicate that it is not a straight average but an average with a weighting function that emphasizes the stress drops near the center of the fault. Thus, an identical concentrated stress applied near the center produces larger slip than it would produce if it were applied near the borders. We may say that the fault is stiffer near the edges and softer near the center.

Using (6) or (7) to obtain the stress drop will yield a weighted average stress drop $\Delta\sigma^*$ which in general will differ from the unweighted average stress drop $\overline{\Delta\sigma}$. However, the weighting function $4/\pi(W^2 - x^2)^{1/2}$ has an elliptical shape which does not deviate much from a constant average. Only in the case of strong stress drop concentration near the edges will $\Delta\sigma^*$ differ significantly from $\overline{\Delta\sigma}$.

3. *Seismic energy*

Traditionally, seismologists have defined the seismic energy E_s as a fraction of the potential energy released by faulting W,

$$E_s = \eta W \tag{9}$$

where η is the seismic efficiency. This relation synthesizes all the dynamic processes of energy release in the efficiency η, which cannot be obtained by purely seismological observations. An expression for E_s in terms of the stresses and slip at the fault was obtained by KOSTROV (1974) and extended recently by DAHLEN (1976) to include the effect of non-elastic prestress fields and rotation of the earth. Here we will derive these relations by a slightly simpler method trying to emphasize the dependence of E_s on the rupture process at every point on the fault.

Let us consider a fault surface $\Sigma(t)$ that grows with time until it reaches its final area Σ_f. The seismic energy is the total flow of elastic energy through a surface S that surrounds the source (Fig. 1). S is sufficiently far from the source that the static field due to the source is negligible. Then the seismic energy is (KOSTROV, 1974).

$$E_s = \int_0^{t^*} dt \int_S dS\, \dot{u}_i\, \Delta\sigma_{ij} n_j \tag{10}$$

where n_j is the normal to S, $\dot{u}_i$ is the particle velocity and $\Delta\sigma_{ij} = \sigma_{ij}(\mathbf{r}, t) - \sigma^0_{ij}(\mathbf{r})$ is the *change* in stress due to the elastic waves. The integral over time is taken until no significant motion arrives from the source.

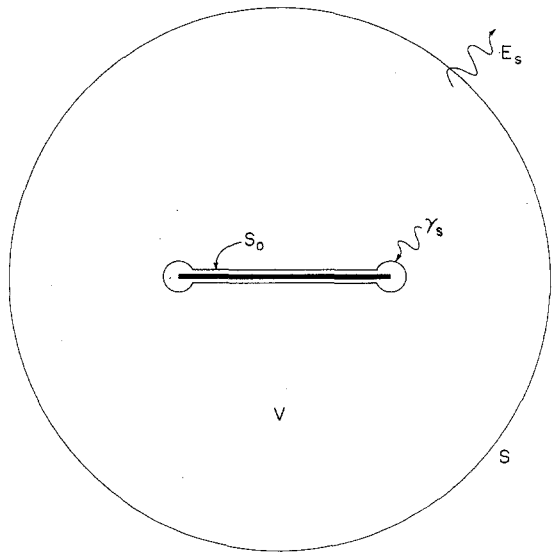

Figure 1
Geometry used to study seismic energy radiation E_s. S is a sphere in the far-field. S_0 is a surface that surrounds all the inelastic zone in the vicinity of the fault. γ_s is the fracture energy absorbed per unit extension of the rupture front.

The definition of E_s in (10) is in terms of stresses and velocities at S and we want to express it in terms of the field at the source. Let us surround the source by a boundary $S_0(t)$ than includes all the non-elastic zone near the fault as shown in Fig. 1. Most of the significant non-linear (plastic) effects occur in a small zone near the fault's edge where large stress concentrations occur. These zones are indicated by the circular indentations near the edges of the fault in Fig. 1. As the fault grows there is irreversible non-elastic energy dissipation in these zones. This energy is used in plastic deformation and in breaking new fault surface. KOSTROV *et al.* (1970) and FREUND (1972) have calculated the energy absorbed and expressed it in terms of the stress concentrations at the crack tip. Here we shall simply designate with γ the energy dissipated per unit advance of the rupture front.

Simple energy balance indicates that the energy flow E_s through S is equal to the energy flow out of the source minus the potential energy change W_s in the elastic volume V and minus the energy absorbed by the fault edge during rupture. Since the problem is linear we proceed by ignoring the pre-stress field and write an energy balance for the dynamic field only. The effect of pre-stress may be included later through interaction energy terms as shown by ESHELBY (1957). We find

$$E_s = \int_0^{t^*} dt \int_{S_0} \dot{D}_i \, \Delta\sigma_{ij} n_j \, dS - W_S - \int_{S_0} \gamma \, dS \tag{11}$$

Where $\dot{D}$ is the slip velocity at the fault, $\Delta\sigma_{ij}$ is the dynamic stress drop and W_s is the potential energy change due to the total stress drop in the absence of pre-stress

$$W_s = \frac{1}{2} \int_{S_0} D_i^f \, \Delta\sigma_{ij}^f n_j \, dS \tag{12}$$

where D_i^f is the final slip at the fault and $\Delta\sigma_{ij}^f$ the final stress drop. In (12) we used the fact that S is sufficiently far from the source so that the static stress field is negligible.

Inserting (12) into (11) we find

$$E_s = \int_0^{t^*} dt \int_{S_0} dS \, \dot{D}_i [\overline{\sigma_{ij}} - \sigma_{ij}(t)] n_j - \int_{S_0} dS\gamma \tag{13}$$

where $\overline{\sigma_{ij}} = 1/2(\sigma_{ij}^0 + \sigma_{ij}^1)$ is the average of the initial stress σ_{ij}^0 and the final stress σ_{ij}^1 at the fault, and $\sigma_{ij}(t)$ is the frictional stress at the fault while slip proceeds ($\dot{D} \neq 0$).

If we assume that the inelastic zones at the edge of the rupture front are small compared to the source dimension then we can rewrite E_s in the form

$$E_s = \int_{S_0} dS \int_0^{D_f} dD_i \, [\overline{\sigma_{ij}} - \sigma_{ij}(D)] n_j - E_{\text{rupt}} \tag{14}$$

where E_{rupt} is the total energy dissipated inelastically at the rupture front. $\sigma(D)$ is the frictional law for slip at each point on the fault. For simplicity we have excluded viscous friction in which case $\sigma(D, \dot{D})$ is also a function of slip velocity. In Fig. 2 we sketch a possible friction law $\sigma(D)$ at a point on the fault and we also indicate the initial (σ^0), final (σ^1) and average ($\bar{\sigma}$) stresses. Also indicated in this figure is the static friction or upper yield point σ^y of the constitutive relation. As suggested by the figure the static friction σ^y may be higher than the initial stress. The increase in stress necessary to produce rupture is provided by dynamic stress concentration ahead of the crack. The history of stress at a point is as follows: first, with the arrival of P and S waves radiated from the nucleation point the stress departs from the initial σ^0 level and as the rupture front gets closer the stress increases. When the stress reaches the level σ^y rupture starts and the stress $\sigma(D)$ decreases as D increases. During the slip, part of the potential energy in the elastic body is released and used to overcome friction, to produce additional fracture and to radiate seismic waves. As indicated by (14) the contribution to E_s from one point on the fault is

$$e_s = \int dD_i [\overline{\sigma_{ij}} - \sigma_{ij}(D)] n_j - \gamma \tag{15}$$

which we may call specific available seismic energy. As seen from Fig. 2 the contribution to e_s is negative for $\sigma(D) > \bar{\sigma}$ and positive for $\sigma(D) < \bar{\sigma}$. The negative contribution is a dissipation and should perhaps, be incorporated into the fracture energy.

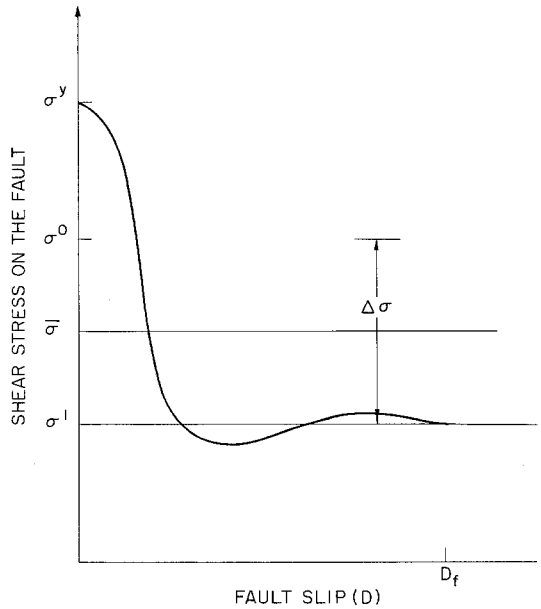

Figure 2
Sketch of a possible frictional low at the fault. σ^y is the yield stress or static friction, σ^0 the initial stress before the nucleation of rupture, σ^1 is the final stress after all motion has ceased, $\bar{\sigma} = \frac{1}{2}(\sigma^0 + \sigma^1)$ is the average stress on the fault. D_f is the total slip.

In fact, IDA (1972) and ANDREWS (1975) have proposed models where there is no inelastic dissipation outside of the fault itself. In this case energy is dissipated at the rupture front only when $\sigma(D) > \bar{\sigma}$. In order to study dynamic faulting problems we have to specify the friction law $\sigma(D)$. This can only be obtained from experiments or, perhaps, eventually inverted from seismic observations. Since we do not know much about $\sigma(D)$ in many dynamical models of source mechanisms a simplified frictional law is used. The assumption is that $\sigma(D)$ drops abruptly to a constant kinetic friction σ^k immediately after slip starts. Some basic considerations of elasticity demonstrate that in this case the stress ahead of the crack has a typical square root singularity and σ^y is necessarily infinite. However the square of the stress intensity factor may be shown to be proportional to the total fracture energy dissipation (KOSTROV *et al.*, 1970, FREUND, 1972). This approximation is well known in fracture mechanics and has been proved to be adequate in most instances.

The frictional law in Fig. 2 is similar to the frictional law proposed by BYERLEE (1970) in his study of the stick-slip instability since, as proposed by BRACE and BYERLEE (1969), the same, or similar, frictional instability may be active in earthquakes as in stick-slip. We can think of an earthquake as a stick-slip instability that propagates on the fault. But there are significant differences between both phenomena due to the dynamic stress concentration that control the spreading of the instability in earthquakes. An important consequence is that the stress drop measured in stick-

slip events is the difference $\delta\sigma = \sigma^y - \sigma^1$ in Fig. 2. In earthquakes, on the other hand, the stress drop $\Delta\sigma$ has to be equal to $\delta\sigma$ only near the rupture nucleation point or at isolated asperities. At other points the stress is driven to the static friction σ^y by the dynamic stress concentrations ahead of the rupture front so that the dynamic stress drop $\delta\sigma$ may be larger than the static stress drop $\Delta\sigma$ determined from (6). This may explain, at least in part, that stress drops measured in the laboratory are significantly larger than the average stress drops obtained for earthquakes.

The seismic energy has been used to obtain the apparent stress (AKI, 1966)

$$\sigma_{\text{app}} = \eta\bar{\sigma} = \mu E_s / M_0 \tag{16}$$

where $\bar{\sigma}$ is the average stress and η the efficiency. This relation has the advantage it does not require an estimate of the source dimensions. E_s is estimated from the energy-magnitude relations so that the estimate (16) may be very rough. Assuming that E_s is well determined we may find an expression for σ_{app} using (14) and (2)

$$\sigma_{\text{app}} = \eta\bar{\sigma} = \frac{1}{\bar{D}S}\int_{S_0} dS \int_0^{D_s} dD_i[\bar{\sigma}_{ij} - \sigma_{ij}(D)]n_j - \frac{\gamma}{D} \tag{17}$$

So that the apparent stress is an average of $\bar{\sigma} - \sigma(D)$ during the fault process. In the case of constant friction $\sigma(D) = \sigma^k$ and (17) reduces to

$$\eta\bar{\sigma} = \frac{1}{S}\int dS[\bar{\sigma} - \sigma^k] - \frac{\gamma}{\bar{D}} \tag{18}$$

a result found also by HUSSEINI (1976). Thus, $\eta\bar{\sigma}$ is not really a measure of absolute stress but, as remarked by SAVAGE and WOOD (1971) and HANKS and THATCHER (1972), $\eta\bar{\sigma}$ is really a measure of stress drop on the fault.

4. *Seismic radiation*

In order to recover stress drops (6 or 7) from seismic observations we need the seismic moment and estimates of the source area and its geometry. For larger earthquakes the area may be estimated from aftershock zones, but for many earthquakes the fault dimensions may only be recovered from the seismic radiation in the time or frequency domain.

Let us consider the radiation of body waves in the far-field and assume that we have removed the effect of the path so that we can treat the source as if it were embedded in an infinite, homogeneous medium. The far-field radiation may be obtained from the representation theorem (BURRIDGE and KNOPOFF, 1964) assuming a planar fault and slip in only one direction

$$u(\mathbf{R}, t) = \frac{\mu}{4\pi\rho c^3} R_{\theta\phi}\frac{1}{R} U_{\text{ff}}(\hat{R}, t - R/c) \tag{19}$$

where, ρ is the density, μ the rigidity and c is either v_p, the P-wave velocity or v_s, the S-wave velocity, $R_{\theta\phi}$ is the double couple radiation pattern, $\hat{R}$ the direction of the observer with respect to a reference point on the source and R is the distance to the observer.

The shape of the far-field pulse is given by

$$U_{\mathrm{ff}}(\hat{R}, \tau) = \iint_S dS\, \dot{D}\left(\mathbf{r}, \tau + \frac{\hat{R}\cdot\mathbf{r}}{c}\right) \tag{20}$$

where $\mathbf{r}$ is a position vector on the fault plane and $\dot{D}(\mathbf{r}, t)$ is the slip velocity distribution on the fault plane. As (20) indicates the far-field pulse is a delayed average of the slip velocity at the source. Since the fault area S_0 is finite and the duration of slip on the source (rise time) is also finite the pulse U_{ff} will have a finite duration. This property is shared by all source models and is used either in the time domain (HASKELL's (1964) model) or in the spectral domain (BRUNE's (1970) model) to retrieve the source dimensions. In order to discuss the spectral properties of the far-field pulse it is convenient to introduce the space and time Fourier transform of the slip velocity function

$$\dot{D}(\mathbf{k}, \omega) = \int_0^\infty dt\, e^{-i\omega t} \int_{S_0} dS\, e^{-i\mathbf{k}\cdot\mathbf{r}}\, \dot{D}(\mathbf{r}, t) \tag{21}$$

Then, transforming (20) we find the following relation between the far-field spectrum and the source slip-velocity spectrum

$$U_{\mathrm{ff}}(\hat{R}, \omega) = \dot{D}(\mathbf{k}, \omega)|_{\mathbf{k}=(R/c)\omega} \tag{22}$$

Expressions similar to this one were obtained by AKI (1967) for linear faults and MADARIAGA (1976) for circular faults.

Many properties of the far-field spectrum may be obtained from (22). For instance, at low frequencies the spectrum is flat and proportional to the seismic moment M_0 (AKI, 1967). Also, as noted by MOLNAR *et al.* (1973b), if $\dot{D}(\mathbf{r}, t)$ is everywhere on the fault of the same sign (unipolar) then the spectral amplitude $|U_{\mathrm{ff}}(\hat{R}, \omega)|$ is maximum at zero frequency, a property disputed by ARCHAMBEAU (1972, 1975). But the property of Fourier transform that interests us the most is that any pulse of finite duration (say ΔT) has a spectrum of finite width (Δf in Hz) such that $\Delta f \Delta t \approx 1$. In seismology it is more common to use the corner frequency in a logarithmic plot of the spectrum (see Fig. 4 and 6) rather than the width of the spectrum. Roughly, the corner frequency, f_0, is one half the spectral width so that $f_0\, \Delta t \approx 0.5$. Thus, the corner frequencies are an inverse measure of the pulse width and, therefore, inversely proportional to some combination of the source size and the rise time. The exact relationship between corner frequency and the source dimensions has to be determined for specific fault models. It will depend on the geometry of the source, the distribution of stress drop on the fault, the presence of multiple sources, vicinity to the free surface, the structure in the vicinity of the source, etc. Little is known about

the effects of these complicating factors. In the following we will concentrate on the discussion of two relatively simple, but quite different geometries, a circular and a rectangular fault.

5. *The circular fault model*

We consider a circular fault that grows symmetrically from a point at a constant rupture velocity v_R and finally stops suddenly at a certain radius a. A kinematic analysis, with arbitrary specification of $\dot{D}(r, t)$ was made by SAVAGE (1966). Later, BRUNE (1970) approximated the dynamic solution assuming that rupture occurred instantaneously on the fault. Recently, we were able to solve this problem numerically (MADARIAGA, 1976). The high degree of symmetry makes this the easiest fault model to study when we specify a constant stress drop on the fault. In order to study the radiation we have to find first the slip function at the source which is the main result of the numerical solution. In Fig. 3 we show the slip history as a function of radius of the fault. This slip function is very approximately cylindrically symmetric, i.e., independent of azimuth. The most important feature of the slip function is that the slip is concentrated near the center of the fault, a result expected from static solutions of circular faults (ESHELBY, 1957). The rise time is also longer near the center of the fault. The slip function shown in Fig. 3 was calculated assuming a constant rupture velocity $v_R = 0.87\, v_S$, v_S = shear velocity. The effect of the rupture velocity is not too severe in the far field radiation of this model because of the great symmetry of

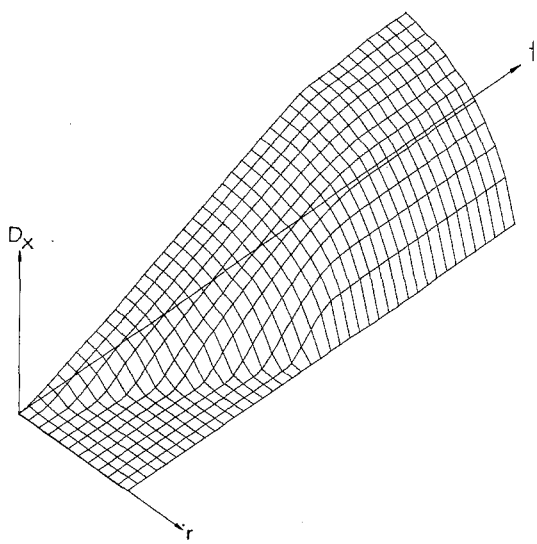

Figure 3
Source slip function for a circular fault with rupture velocity $v_R = 0.87\, v_s = 0.5\, v_p$. This plot shows the slip history as function of radius on the fault.

the fault and the fact that most of the radiation comes from stopping phases generated during the abrupt stopping of rupture at the final radius (a). Thus varying the rupture velocity within reasonable limits – say $v_R = 0.6$–$0.9\ v_S$ – does not affect the radiation significantly.

Far-field radiation from the circular model was obtained by a series of Fourier transforms and a relation of the type of (22). In Fig. 4 we show an example of the far-field displacement pulse radiated in a direction $\theta = 60°$ from the normal to the fault. Radiation is symmetrical about this normal. The shape of the far-field pulse and spectra change very slowly as a function of θ; $\theta = 60°$ may be considered as an 'average' radiation. From Fig. 4 we see that the spectral amplitude has a characteristic corner frequency f_0 defined by the intersection of the low and high frequency asymptotes. We find that the corner frequency, averaged for different rupture velocities and azimuth, has the following relation to the source radius

$$f_0^P = 0.32\ v_s/a$$
$$f_0^S = 0.21\ v_s/a \tag{23}$$

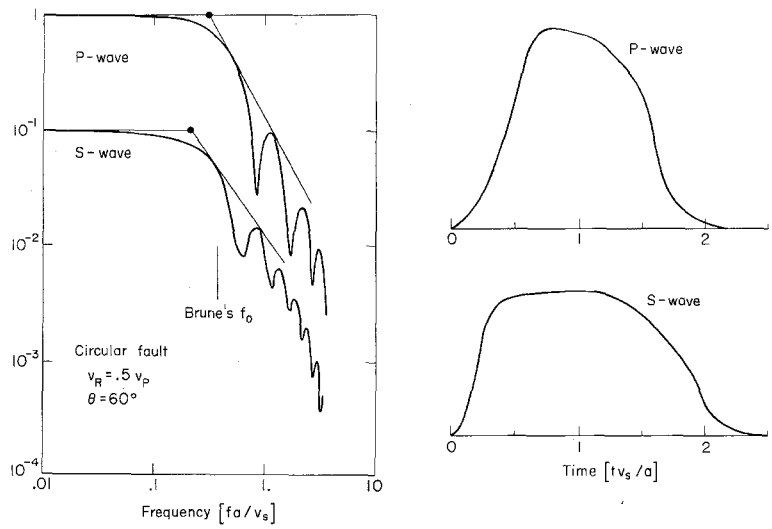

Figure 4

Far-field P and S pulses and their spectra radiated by the circular fault whose source slip function is shown in Fig. 3. The spectrum of P waves is normalized to 1 at low frequencies. The spectrum of S waves is normalized to 0.1 at low frequencies. Both pulses are normalized to the same seismic moment (area).

for P and S waves respectively. BRUNE (1970) proposed a coefficient 0.375 for S waves. We notice that the P-wave corner is at higher frequency than the S-corner frequency, a relation that has been observed in many earthquake spectra as shown by MOLNAR *et al.* (1973a). Higher P-corner frequencies are a property of faults of low length-to-width ratio. It is interesting to note that the corner of the displacement amplitude spectrum is very approximately the peak frequency of the energy density

spectrum. That is, the corner defines the frequency at which the source is more efficient in transferring power to the far-field radiation. The wavelengths associated with the corner frequencies are $\lambda^P = 5.41a$ for P-waves and $\lambda^S = 4.76a$ for S-waves. Thus, the circular source has a maximum efficiency to transfer energy at wavelengths of about 2.5 times the source diameter.

6. *Rectangular fault model*

The rectangular fault model was the first source model studied by seismologists (BEN-MENAHEM, 1961, HASKELL, 1964). Rupture nucleates instantaneously across the width of the fault and then extends longitudinally at a constant rupture velocity v_R either unilaterally or bilaterally until it stops abruptly. In this model the nucleation and stopping of rupture are not considered in detail so that the model is valid only down to wavelengths of the order of the width of the fault. The original studies of this model were purely kinematical, i.e., stress plays no role, assuming a propagating ramp dislocation. We have studied this problem numerically (MADARIAGA, 1977) assuming a constant stress drop on the fault in order to find a dynamically acceptable source time function and slip distributions across the fault. In Fig. 5 we show the source time function along the longitudinal axis of a rectangular fault model of length-to-width ratio $L/W = 3$. Rupture velocity is $v_R = 0.9\, v_S$ and slip is longitudinal (strike slip). The source time function is quite different from that of the

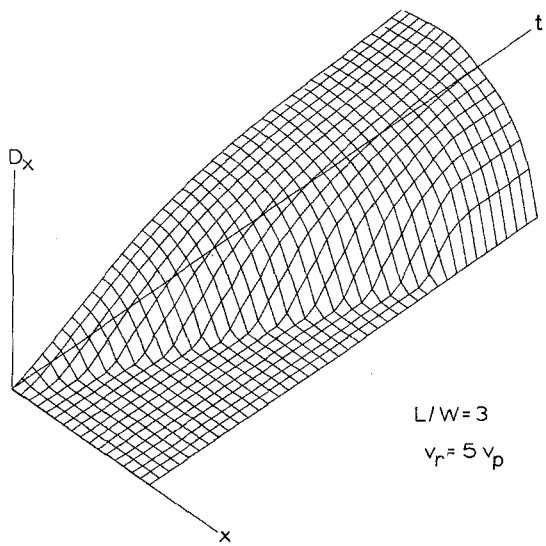

Figure 5
Source slip function for a rectangular fault with bilateral rupture velocity $v_R = 0.87\, v_s = 0.5\, v_p$. This plot shows the slip history for several points along the longitudinal axis of the fault. The length to width ratio of this fault is $L/W = 3$.

circular fault, the slip history is approximately the same along the fault substantiating the kinematic models in which the source was modelled as a propagating dislocation. The slip function at a point, however, differs markedly from a ramp, being sharply rounded near the rupture front. The rise time is approximately a constant along the fault, $T_R = 1.3\, w/v_S$ in contrast to the circular fault where the rise time was longer at the center. In a long fault two patches of rupture move away from the nucleation point leaving a healed fault in their wake. This produces strong focussing of the radiation in directions along the axis of the fault. In contrast a circular fault focuses energy in the direction normal to its plane.

In Fig. 6, we show far-field pulses and spectra radiated by a bilateral crack ($L/W = 3, v_R = 0.5\, v_S$) for a direction that makes an angle $\psi = 58°$ with the longitudinal axis of the fault. This is a representative or 'average' direction of radiation. The most noticeable difference with radiation from a circular fault is that the far-field pulse is more complex. There seem to be two distinct pulses, the longer one, of smaller amplitude is due to radiation from the rupture front that moves away from the observer, while the shorter, stronger initial pulse is associated with the rupture moving towards the observer. The spectra are correspondingly more complicated and in Fig. 6 there seem to be two obvious corner frequencies. The lower corner is associated with longitudinal propagation, while the higher corner is associated with the width and rise time of the fault. It is difficult to establish a simple relationship between corner frequency and source length because the rupture velocity affects the corner frequencies markedly and the spectra are very sensitive to the angle of

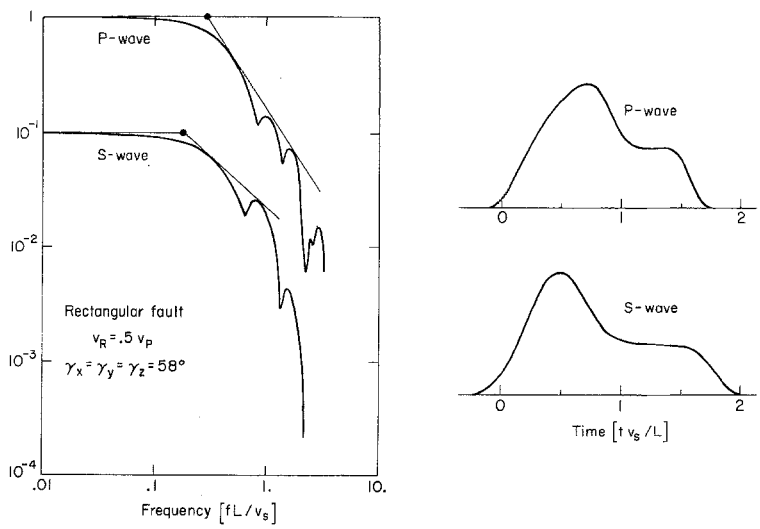

Figure 6
Far-field P and S pulses and their spectra radiated by the rectangular fault of Fig. 5. The spectra and pulses are normalized in the same manner as those in Fig. 4.

radiation. Tentatively, for $v_R = 0.9\, v_S$ we propose, on the average,

$$f_0^P = 0.29\, v_s/L$$
$$f_0^S = 0.20\, v_s/L \tag{24}$$

This problem is further discussed in MADARIAGA (1977).

The rectangular fault model is much more complex than the circular fault model in its dynamics. The two scales of the model, length and width affect different regions of the spectrum and, as a consequence, we expect at least two corner frequencies. In order to obtain an estimate of the stress drop from (6) it is necessary to find both the length and the width from the far-field radiation. This is a very difficult observational problem which may be feasible for only a few large earthquakes. For smaller earthquakes at most one corner frequency may be retrieved from the spectrum or, equivalently, not more than the pulse width may be obtained from the far-field radiation. It appears that information not contained in the spectra, like aftershock distribution, is necessary to establish the width of the fault and then estimate the stress drop. Many authors assume that the fault is circular and proceed to find the stress drop from (7) rather than (6). If the fault happened to be elongated, this procedure would produce large errors because the stress drop in (6) is inversely proportional to the square of the fault width.

7. *Discussion*

We have reviewed the results of attempts to model earthquake sources as mechanical instabilities caused by a drop in the ability to sustain stress on a plane fault. The models studied are highly idealized because the mathematical problems that arise even with the simplest fault models make it necessary to use expensive numerical methods. Moreover, fault radiation requires the use of three dimensional models because of the significant geometrical effects that appear in elongated faults. In a discussion of the estimate of stress drop (equation 6) by usual methods we have emphasized that the fault geometry is an important variable that is not usually incorporated in the inversion of stress drop from seismic observations. These geometrical effects were shown to dominate the slip history and radiation from the two simple source models that we discussed – a circular fault and a rectangular fault. Using the wrong fault model for a given earthquake may generate large errors in the inversion of stress drop.

We have also discussed the role of the frictional law in the modelling of earthquake sources. This frictional law is largely unknown but we have argued that it should be similar to the frictional law in laboratory stick-slip experiments. One significant property of dynamical source models is the presence of stress concentrations ahead of the rupture front. These stress concentrations are purely dynamical effects which

are absent from frictional experiments in the laboratory. As a consequence the dynamic stress drop (which should be equal to stress drop in stick-slip) may be larger than the static stress drops obtained by seismologists. The seismic stress drops are thus lower bounds to the actual dynamic stress drops.

Acknowledgements

This work was supported by the Division of Earth Sciences of the National Science Foundation under Grant EAR75–14808 A01.

References

AKI, K. (1966), *Generation and propagation of G waves from the Niigata earthquake of June 16, 1964, 2, Estimation of earthquake moment, released energy, and stress-strain drop from G-wave spectrum,* Bull. Earthquake Res. Inst. Tokyo Univ. *44*, 73–88.

AKI, K. (1967), *Scaling law of seismic spectrum,* J. Geophys. Res. *72*, 1217–1231.

ANDREWS, D. J. (1976), *Rupture propagatian with finite strain in antiplane strain,* J. Geophys. Res. *81*, 3575–3582.

ARCHAMBEAU, C. B. (1972), *The theory of stress wave radiation from explosions in prestressed media,* Geophys. J. *29*, 329–366.

ARCHAMBEAU, C. (1975), *Developments in seismic source theory,* Rev. Geophys. Space Phys. *13*, 304–306.

ARCHULETA, R. J. and FRAZIER, G. A. (1976), *A three dimensional, finite element solution in a half space for the near field motion of a propagating stress drop* (abstract), Earthquake Notes *47*, 37–38.

BEN-MENAHEM, A. (1962), *Radiation of seismic body waves from a finite moving source in the earth,* J. Geophys. Res. *67*, 345–350.

BRACE, W. F. and BYERLEE, J. D. (1966), *Stick-slip as a mechanism for earthquakes,* Science, *153*, 990–992.

BRUNE, J. N. (1970), *Tectonic stress and the spectra of seismic shear waves from earthquakes,* J. Geophys. Res. *75*, 4997–5009.

BURRIDGE, R. and KNOPOFF, L. (1964), *Body force equivalents for seismic dislocations,* Bull. Seism. Soc. Am. *54*, 1875–1888.

BYERLEE, J. D. (1970), *The mechanics of stick-slip,* Tectonophysics, *9*, 475–486.

CHERRY, J. T., BACHE, T. C. and MASSO, J. F. (1976), *A three dimensional finite-difference simulation of earthquake faulting* (abstract), EOS, Trans. Am. Geophys. Un. *57*, 281.

DAHLEN, F. A. (1976), *Seismic faulting in the presence of a large compressive stress,* Geophys, Res. Lett. *3*, 245–248 and 506.

ESHELBY, J. D. (1957), *The determination of the elastic field of an ellipsoidal inclusion, and related problems,* Proc. Roy. Soc. *A241*, 376–396.

FREUND, L. B. (1972), *Energy flux into the tip of an extending crack in an elastic solid,* J. Elasticity, *2*, 341–348

HANKS, T. C. and THATCHER, W. (1972), *A graphical representation of seismic sources,* J. Geophys. Res. *77*, 4393–4405.

HASKELL, N. A. (1964), *Total energy and energy spectral density of elastic wave radiation from propagating faults,* Bull. Seism. Soc. Am. *54*, 1811–1841.

HUSSEINI, M. I. (1976), *Energy balance for motion along a fault,* submitted to Geophys. J. Roy. astr. Soc.

IDA, Y. (1972), *Cohesive force across the tip of a longitudinal shear crack and Griffith's specific surface energy,* J. Geophys. Res. *77*, 3796–3805.

KANAMORI, H. and ANDERSON, D. L. (1975), *Theoretical basis of some empirical relations in seismology,* Bull. Seism. Soc. Am. *65*, 1073–1095.

KEILIS-BOROK, V. I. (1959), *On the estimation of the displacement in an earthquake source and of source dimensions,* Ann. Geofis. *12*, 205–214.

KNOPOFF, L. (1958), *Energy release in earthquakes,* Geophys. J. *1*, 44–52.

KOSTROV, B. V. (1974), *Seismic moment and energy of earthquakes, and seismic flow of rock,* Izv. Fizika Zemli, *1*, 23–40.

KOSTROV, B. V. and NIKITIN, L. V. (1970), *Some general problems of mechanics of brittle fracture*, Arch. Mech. Stosow., *22*, 749–776.

MADARIAGA, R. (1976), *Dynamics of an expanding circular fault,* Bull. Seism. Soc. Am. **65**, 163–182.

MADARIAGA, R. (1977), *A dynamic stress drop model of a rectangular fault,* in preparation.

MOLNAR, P., TUCKER, B. and BRUNE, J. N. (1973a), *Corner frequencies of P and S waves and models of earthquake sources,* Bull. Seism. Soc. Am. *65*, 2091–2104.

MOLNAR, P., JACOB, K. H. and MCCAMY, K. (1973b), *Implications of Archambeau's earthquake source theory for slip on fault,* Bull. Seism. Soc. Am. *63*, 101–104.

SAVAGE, J. C. (1966), *Radiation from a realistic model of faulting,* Bull. Seism. Soc. Am. *56*, 577–592.

SAVAGE, J. C. and WOOD, M. D. (1971), *The relation between apparent stress and stress drop,* Bull. Seism. Soc. Am. *61*, 1381–1388.

SNEDDON, I. N. and LOWENGRUB, M. (1962), *Crack problems in the classical theory of elasticity*, (John Wiley and Sons, New York.

THATCHER, W. and HANKS, T. (1973), *Source parameters of southern California earthquakes,* J. Geophys. Res. *78*, 8547–8576.

(Received 4th November 1976)